Size-dependent electron-hole exchange interaction in Si nanocrystals

M. L. Brongersma,[a] P. G. Kik, and A. Polman
FOM Institute for Atomic and Molecular Physics, Kruislaan 407, 1098 SJ Amsterdam, The Netherlands

K. S. Min and Harry A. Atwater
Thomas J. Watson Laboratory of Applied Physics, California Institute of Technology, Pasadena, California 91125

Silicon nanocrystals with diameters ranging from ≈ 2 to 5.5 nm were formed by Si ion implantation into SiO_2 followed by annealing. After passivation with deuterium, the photoluminescence (PL) spectrum at 12 K peaks at 1.60 eV and has a full width at half maximum of 0.28 eV. The emission is attributed to the recombination of quantum-confined excitons in the nanocrystals. The temperature dependence of the PL intensity and decay rate at several energies between 1.4 and 1.9 eV was determined between 12 and 300 K. The temperature dependence of the radiative decay rate was determined, and is in good agreement with a model that takes into account the energy splitting between the excitonic singlet and triplet levels due to the electron-hole exchange interaction. The exchange energy splitting increases from 8.4 meV for large nanocrystals (≈ 5.5 nm) to 16.5 meV for small nanocrystals (≈ 2 nm). For all nanocrystal sizes, the radiative rate from the singlet state is 300–800 times larger than the radiative rate from the triplet state. © *2000 American Institute of Physics.* [S0003-6951(00)04402-8]

Si nanostructures have received intense study, which is stimulated by their potential for use in Si-based optoelectronic devices.[1,2] The photoluminescence (PL) from Si nanostructures that are well passivated by H or SiO_2 is attributed to the recombination of quantum-confined excitons.[3–6] The nanocrystals show a higher quantum efficiency for optical emission than bulk Si,[4] and exhibit a band gap (emission energy) that can be continuously tuned over a large part of the visible spectrum and to the near infrared, by varying the size.[7] One of the most controlled methods to fabricate Si nanocrystals in SiO_2 is ion beam synthesis.[8–10] Si nanocrystals formed by this method provide an ideal system for the study of their size-dependent optical properties since the nanocrystals (1) generally have a wide size distribution, (2) are all close to spherical in shape, and (3) are well passivated by the SiO_2 matrix. Si nanocrystal-doped SiO_2 films made by ion beam synthesis show PL that can be attributed to two distinct sources.[8] One luminescence feature is due to ion irradiation-induced defects and can be fully quenched by introducing H or D into the film. The other is attributed to the recombination of quantum-confined excitons.

In this letter, we present temperature-dependent measurements of the PL intensity and PL decay rate of ion beam synthesized Si nanocrystals in the size range of ≈ 2–5.5 nm. The temperature dependence of the radiative decay rate of Si nanocrystals is determined and compared to a model introduced by Calcott *et al.*,[6] that takes into account the exchange interaction splitting of the singlet and triplet exciton energy levels.[3,6] The exchange splitting energy is determined as a function of emission energy in the spectral range 1.4–1.9 eV, and compared to data for porous Si for energies >1.8 eV. The ratio of the singlet and triplet radiative decay rates is determined for the first time.

A 100 nm thick SiO_2 film grown by wet thermal oxidation of a lightly B-doped Si(100) wafer was implanted at room temperature with 50 keV Si ions at a fluence of 5×10^{16} Si/cm^2. The sample was subsequently annealed at 1100 °C for 10 min in vacuum to induce nucleation and growth of Si nanocrystals. The presence of close to spherical Si nanocrystals was confirmed by transmission electron microscopy. Finally, the SiO_2 film was implanted with 3.3×10^{15} D/cm^2 at an energy of 600 eV to quench the defect luminescence.[8] PL spectra were taken using excitation with the 459 nm line of an Ar-ion laser at a power density of ~ 1 mW/mm^2. Lock-in detection was performed at a frequency of 16 Hz. The luminescence was detected with an InGaAs photomultiplier and a grating spectrometer. The sample temperature was controlled between 12 and 300 K in a closed-cycle He cryostat. All spectra were corrected for the system response. PL decay measurements were made after pumping to steady state with a power density of ~ 0.2 mW/mm^2. The time resolution of the system was 400 ns.

Figure 1 shows PL spectra taken at 12, 100, and 300 K. The spectrum at 12 K is broad (full width at half maximum 0.28 eV) and peaks around 1.6 eV. When the temperature is raised, the peak intensity increases with temperature up to 100 K and decreases again for higher temperatures. A shift of the peak position to lower energies is observed when the temperature is increased to 300 K, while the overall spectral shape hardly changes.

The spectrum is broad due to the wide distribution of nanocrystal sizes, each emitting at their characteristic, size-dependent energy. The full spectral range from 1.4 to 2.0 eV corresponds to a size range of about 5.5–2 nm.[11] The inset in Fig. 1 shows the dependence of the peak position on temperature as obtained from PL spectra taken at various temperatures in the range from 12 to 300 K. The peak energy decreases monotonically from 1.60 to 1.54 eV as the tem-

---

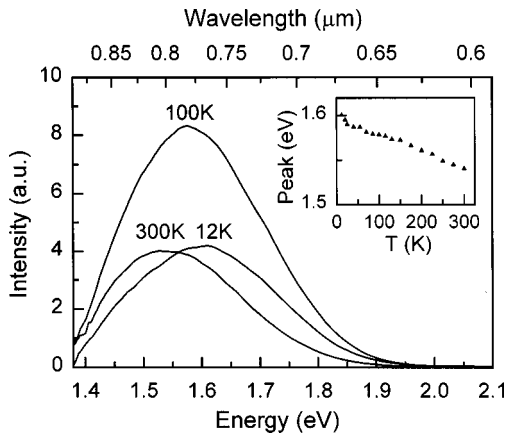[a] Electronic mail: mbrong@caltech.edu

FIG. 1. Photoluminescence spectra taken at 12, 100, and 300 K of a 100 nm thick SiO$_2$ film that contains ion beam synthesized Si nanocrystals with a broad size distribution. The inset shows the peak energy of these and other spectra (not shown) taken at various temperatures. Excitation at 458 nm (2.71 eV) and a power density of $\approx$1 mW/mm^2.

perature is increased from 12 to 300 K. The decrease can mainly be attributed to the decrease in the band gap energy with temperature. For comparison: the band gap variation with temperature for bulk Si is 50 meV over the temperature range from 10 to 300 K.

Figure 2(a) shows the dependence of the integrated PL intensity on temperature. It first increases by a factor of 2 from 12 to 100 K and then decreases by a similar amount when the temperature is increased to 300 K. The fact that the PL spectrum does not change shape, but shifts with increasing temperature, suggests that the temperature dependence of the emission intensity is the same for all nanocrystal sizes that contribute to the spectrum.

PL decay traces at emission energies of 1.46, 1.55, 1.65, 1.77, and 1.90 eV were measured at temperatures in the range from 12 to 300 K. The decay traces are well described by a stretched exponential function,

$$I_{PL}(t) = I_0 \exp[-(R_{PL}t)^\beta], \tag{1}$$

where I_0 is the PL intensity at $t=0$, R_{PL} an effective decay rate, and β a constant between 0 and 1. A typical decay trace taken at 1.65 eV and 15 K is shown in the inset of Fig. 2(b). For this trace $R_{PL}=6.2\times10^2$ s^{-1} ($1/R_{PL}=1.6$ ms) and $\beta=0.65$. Figure 2(b) shows the temperature dependence of R_{PL}, as obtained by fitting the decay traces taken at 1.46 (dots), 1.65 (squares), and 1.90 eV (triangles) with Eq. (1). The drawn lines serve to guide the eye. At each energy, R_{PL} first increases rapidly by more than an order of magnitude between 12 and 90 K, and then slowly up to 300 K.

The temperature dependence of I_{PL} and R_{PL} [Figs. 2(a) and 2(b)] can be described by a model[3,6] that ascribes the luminescence to the recombination of strongly localized excitons in crystalline Si (see inset in Fig. 3). In this model, the excitonic levels are split by an energy, Δ, due to the exchange interaction between the electron and hole. The lower level corresponds to a triplet state which is threefold degenerate and has a radiative decay rate R_T. The upper level corresponds to a singlet state and has a radiative decay rate R_S. This simple two-level model has been used to describe the temperature-dependent luminescence of porous silicon. There is some conflict in the literature whether this model,
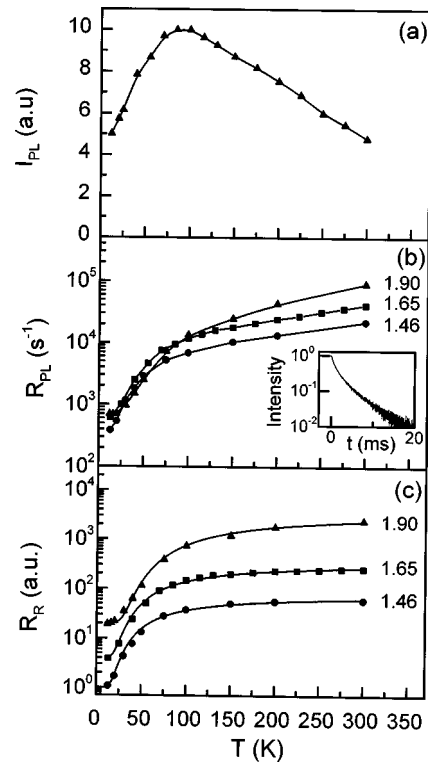

FIG. 2. (a) Temperature dependence of the integrated photoluminescence intensity, I_{PL}, of Si nanocrystals in SiO$_2$. (b) Temperature dependence of the photoluminescence decay rate, R_{PL}, measured at emission energies of 1.46, 1.65, and 1.90 eV. The inset shows a typical decay trace taken at 1.65 eV and 15 K. (c) Temperature dependence of the radiative rate at emission energies of 1.46, 1.65, and 1.90 eV, obtained from a multiplication of the temperature dependent I_{PL} data in (a) and R_{PL} data in (b). The solid curves are best fits of R_R using a model that takes into account the exchange splitting of the energy levels of quantum-confined excitons in the Si nanocrystals.

that applies for nonspherical particles, would apply for spherical nanocrystals as well.[12–14] In any case, the exact shape of our ion beam synthesized nanocrystals is unknown and may in fact be slightly nonspherical.

The temperature dependence of the total radiative decay rate, R_R, can be calculated by assuming thermal equilibrium between the two levels:

$$R_R = \frac{3R_T + R_S \exp(-\Delta/kT)}{3 + \exp(-\Delta/kT)}. \tag{2}$$

In general, the radiative decay competes with nonradiative decay channels (at a rate R_{NR}) that can, for example, be provided by defects in the nanocrystal itself or at the Si/SiO$_2$ interface. At low pump power density, the decay of excited electron hole pairs is unimolecular and $R_{PL}=R_R+R_{NR}$. In low-power steady state conditions, I_{PL} is proportional to the quantum yield, $\eta = R_R/(R_R+R_{NR})$. Therefore, by calculating the product of the measured I_{PL} and R_{PL} at each temperature, a relative measure can be derived of the temperature dependence of the *radiative decay rate R_R*.

Figure 2(c) shows the calculated temperature dependence of R_R for emission energies of 1.46, 1.65, and 1.90 eV, obtained from a multiplication of I_{PL} [Fig. 2(a)] and R_{PL} [Fig. 2(b)] at each temperature. Since these data are derived from the unnormalized I_{PL}, each data set is expressed in arbitrary units, and has been multiplied by a different con-
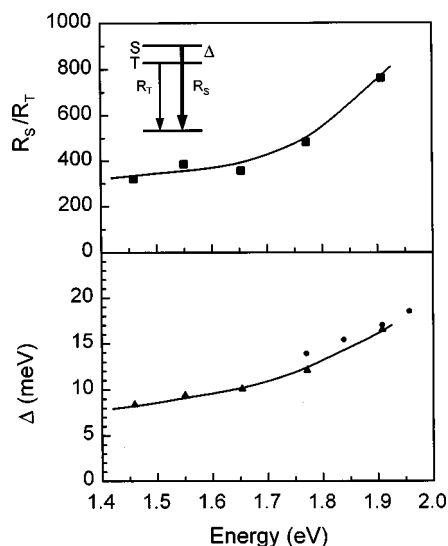
FIG. 3. (a) Ratio of the singlet (R_S) and triplet (R_T) radiative decay rates of quantum-confined excitons in Si nanocrystals as a function of the emission energy. The inset shows a schematic of the singlet and triplet energy levels, split by the electron-hole exchange energy Δ. (b) Exchange energy as a function of the emission energy. The triangles are obtained from the measurements described in this letter. The dots represent values of Δ obtained for porous Si taken from Ref. 6. The values of R_S/R_T and Δ were determined by fitting Eq. (2) to the temperature dependence of the radiative rate shown in Fig. 2(c).

stant factor to facilitate comparison. The data in Fig. 2(c) can now be fitted with Eq. (2) and the drawn lines show the resulting fits. The temperature dependence of R_R is in excellent agreement with this model. At low temperature ($T \approx 12$ K and $kT \approx 1.0$ meV), only the triplet state is occupied and the radiative decay rate is small. The radiative decay rate of a pure triplet state should be zero as the transition is parity forbidden. However, the spin-orbit interaction slightly mixes the singlet and triplet states, making the transition weakly allowed. At higher temperatures, the singlet state becomes populated and the radiative rate increases by more than an order of magnitude between 12 and 100 K. When the temperature is increased further, the population in the singlet state converges to its high temperature value which is 1/3 of the total triplet population, and R_R is dominated by R_S. Indeed, R_R shows only a small variation with temperature for $T > 100$ K. The data for 1.46, 1.65, and 1.90 eV show a slightly different behavior which can be explained by differences in the values of R_T, R_S, and Δ, as will be shown below.

Figure 3(a) shows the ratio of R_S to R_T as a function of emission energy obtained by fitting Eq. (2) to the temperature dependent data of R_R shown in Fig. 2(c) and to data taken at other energies (not shown). At all energies, R_S is 300–800 times larger than R_T. The triangles in Fig. 3(b) show the dependence of the exchange splitting energy, Δ, on the emission energy, E. The value of Δ increases from 8.4 to 16.5 meV between $E = 1.46$ and 1.90 eV, corresponding to a

nanocrystal size range of ≈ 5.5–2 nm. For reference, we also plot values obtained for porous Si for $E = 1.7$ to 2.0 eV.[3,6] These measurements cannot be directly compared to those presented in this letter, as the nanostructures in porous Si are irregularly shaped, and surrounded by an inhomogeneous dielectric, in contrast to the case for the roughly spherical nanocrystals in an SiO_2 matrix in this letter. Still, the data for porous Si seem to follow the trend suggested by our data. This suggests that the magnitude of Δ is basically related to the emission energy. For a spherical crystallite with a diameter of 3 nm (emission energy ≈ 1.8 eV), effective mass theory predicts $\Delta = 13.9$ meV,[3] in good agreement with the data in Fig. 3(b). The values of Δ found here are much smaller than the 71 meV that was reported earlier for oxidized Si nanocrystals.[15] In that case, however, the luminescence was thought to originate from states at the Si/SiO_2 surface.

In conclusion, the temperature dependence of the photoluminescence intensity and decay rate of excitons in Si nanocrystals was studied. The data are in agreement with a model that takes into account the size-dependent exciton exchange splitting between the singlet and triplet states. The exchange energy splitting was found to increase from 8.4 meV for the large nanocrystals (≈ 5.5 nm) to 16.5 meV for small nanocrystals (≈ 2 nm). For all nanocrystal sizes, the radiative rate from the singlet state is 300–800 times larger than the radiative rate from the triplet state.

[1] K. D. Hirschman, L. Tsybeskov, S. D. Duttagupta, and P. M. Fauchet, Nature (London) **384**, 338 (1996).

[2] Y. Kanemitsu, Phys. Rep. **263**, 1 (1995).

[3] P. D. J. Calcott, K. J. Nash, L. T. Canham, M. J. Kane, and D. Brumhead, J. Phys.: Condens. Matter **5**, L91 (1993); A. G. Cullis, L. T. Canham, and P. D. J. Calcott, J. Appl. Phys. **82**, 909 (1997).

[4] L. E. Brus, P. F. Szajowski, W. L. Wilson, T. D. Harris, S. Schuppler, and P. H. Citrin, J. Am. Chem. Soc. **117**, 2915 (1995).

[5] S. Schuppler, S. L. Friedman, M. A. Marcus, D. L. Adler, Y. H. Xie, F. M. Ross, T. D. Harris, W. L. Brown, Y. J. Chabal, L. E. Brus, and P. H. Citrin, Phys. Rev. Lett. **72**, 2648 (1994).

[6] P. D. J. Calcott, K. J. Nash, L. T. Canham, M. J. Kane, and D. Brumhead, J. Lumin. **57**, 257 (1993).

[7] M. L. Brongersma, A. Polman, K. S. Min, E. Boer, T. Tambo, and H. A. Atwater, Appl. Phys. Lett. **72**, 2577 (1998).

[8] K. S. Min, K. V. Shcheglov, C. M. Yang, H. A. Atwater, M. L. Brongersma, and A. Polman, Appl. Phys. Lett. **69**, 2033 (1996).

[9] J. Linnros, A. Galeckas, N. Lalic, and V. Grivickas, Thin Solid Films **297**, 167 (1997).

[10] M. L. Brongersma, A. Polman, K. S. Min, and H. A. Atwater, J. Appl. Phys. **86**, 759 (1999).

[11] R. T. Collins, P. M. Fauchet, and M. Tischler, Phys. Today **50**, 24 (1997).

[12] E. Martin, C. Delerue, G. Allan, and M. Lannoo, Phys. Rev. B **50**, 18258 (1994).

[13] A. L. Efros, M. Rosen, M. Kuno, M. Nirmal, D. J. Norris, and M. Bawendi, Phys. Rev. B **54**, 4843 (1996).

[14] K. Leung and K. B. Whaley, Phys. Rev. B **56**, 7455 (1997).

[15] Y. Kanemitsu, Phys. Rev. B **53**, 13515 (1996).